

RESEARCH ARTICLE

# Withaferin A Induces ROS-Mediated Paraptosis in Human Breast Cancer Cell-Lines MCF-7 and MDA-MB-231

Kamalini Ghosh, Soumasree De, Sayantani Das, Srimoyee Mukherjee, Sumita Sengupta Bandyopadhyay\*

Department of Biophysics, Molecular Biology and Bioinformatics, University of Calcutta, India

\* [bandyopas@gmail.com](mailto:bandyopas@gmail.com)



**OPEN ACCESS**

**Citation:** Ghosh K, De S, Das S, Mukherjee S, Sengupta Bandyopadhyay S (2016) Withaferin A Induces ROS-Mediated Paraptosis in Human Breast Cancer Cell-Lines MCF-7 and MDA-MB-231. PLoS ONE 11(12): e0168488. doi:10.1371/journal.pone.0168488

**Editor:** Aamir Ahmad, University of South Alabama Mitchell Cancer Institute, UNITED STATES

**Received:** June 20, 2016

**Accepted:** November 30, 2016

**Published:** December 29, 2016

**Copyright:** © 2016 Ghosh et al. This is an open access article distributed under the terms of the [Creative Commons Attribution License](https://creativecommons.org/licenses/by/4.0/), which permits unrestricted use, distribution, and reproduction in any medium, provided the original author and source are credited.

**Data Availability Statement:** All relevant data are within the paper and its Supporting Information files.

**Funding:** This work was supported by grants from DST (SR/SO/BB-58/2007), UGC (UGC-37-398/2009) to SS(B), UGC-DSA. We would like to acknowledge for providing fellowship to KG (UGC-RFSMS and ICMR), SM (UGC-RFSMS), S. De (CSIR), S. Das (CSIR). Indian Council of Medical research (Sanction No: 45/57/2009/BMS/TRM) for funding.

## Abstract

Advancement in cancer therapy requires a better understanding of the detailed mechanisms that induce death in cancer cells. Besides apoptosis, the mode of other types of cell death has been increasingly recognized in response to therapy. Paraptosis is a non-apoptotic alternative form of programmed cell death, morphologically distinct from apoptosis and autophagy. In the present study, Withaferin-A (WA) induced hyperpolarization of mitochondrial membrane potential and formation of many cytoplasmic vesicles. This was due to progressive swelling and fusion of mitochondria and dilation of endoplasmic reticulum (ER), forming large vacuolar structures that eventually filled the cytoplasm in human breast cancer cell-lines MCF-7 and MDA-MB-231. The level of indigenous paraptosis inhibitor, Alix/AIP-1 (Actin Interacting Protein-1) was down-regulated by WA treatment. Additionally, prevention of WA-induced cell death and vacuolation on co-treatment with protein-synthesis inhibitor indicated requirement of *de-novo* protein synthesis. Co-treatment with apoptosis inhibitor resulted in significant augmentation of WA-induced death in MCF-7 cells, while partial inhibition in MDA-MB-231 cells; implying that apoptosis was not solely responsible for the process. WA-mediated cytoplasmic vacuolation could not be prevented by autophagy inhibitor wortmannin as well, claiming this process to be a non-autophagic one. Early induction of ROS (Reactive Oxygen Species) by WA in both the cell-lines was observed. ROS inhibitor abrogated the effect of WA on: cell-death, expression of proliferation-associated factor and ER-stress related proteins, splicing of XBP-1 (X Box Binding Protein-1) mRNA and formation of paraptotic vacuoles. All these results conclusively indicate that WA induces death in both MCF-7 and MDA-MB-231 cell lines by ROS-mediated paraptosis.

## Introduction

Programmed Cell Death (PCD) has been classified into different types based on the biochemical and morphological characteristics of the cells under different pathological and physiological conditions. Type I PCD or apoptosis has been associated with nuclear cell death, which can operate in a caspase-dependent manner [1]. Apoptosis was considered the only way of cancer

**Competing Interests:** The authors have declared that no competing interests exist.

**Abbreviations:** Z-vad-fmk, N-Benzyloxycarbonyl-Val-Ala-Asp(O-Me) fluoromethylketone;  $\Delta\psi_m$ , Mitochondrial membrane potential; WT, Wortmannin; XBP1, X box-binding protein 1; TMRE, Tetramethylrhodamine ethyl ester; H<sub>2</sub>DCFDA, 2', 7'-dichlorodihydrofluorescein diacetate; GAPDH, Glyceraldehyde-3-phosphate dehydrogenase; FITC, Fluorescein isothiocyanate; AIP-1, Actin-interacting protein 1; DMEM, Dulbecco's Modified Eagle's medium; FBS, Fetal bovine serum; HRP, Horseradish peroxidase; EtBr, Ethidium bromide; PAGE, Polyacrylamide gel electrophoresis; PCR, Polymerase chain reaction; PCNA, Proliferating cell nuclear antigen; GRP78, Glucose-regulated protein, 78kDa; CHOP, C/EBP-homologous protein; DMSO, Dimethyl sulfoxide.

cell death in the past, but the role of other cellular death mechanisms are being increasingly recognized in response to tumor therapy [2]. Type II PCD or autophagic cell death is mediated by sequestration of cytoplasmic organelles in double or multi-membrane autophagic vesicles and subsequent lysosomal degradation [3]. Type III PCD, characterized by cytoplasmic cell death with non-lysosomal vesiculate [4], also known as paraptosis is a non-apoptotic alternative form of programmed cell death that is 'related to apoptosis' but lacks the features that are characteristic of apoptosis (e.g., nuclear fragmentation, chromatin condensation and the formation of apoptotic bodies) and is insensitive to a broad range of caspase inhibitors [5,6]. The molecular mechanisms of paraptosis induction are not yet well defined. Cross-talk between cell death signaling pathways may allow cells to switch between different mechanisms of PCD. They can activate in parallel and interact [7].

Withaferin A (WA), a naturally occurring steroidal lactone which is derived from the root of *Withaniasomnifera Dunal* (WS) or Ashwagandha, one of the most ancient herbs used in traditional Indian ayurvedic medicine for centuries. Several studies have already demonstrated it as a potent anti-angiogenic agent in a variety of human cancer cells by targeting numerous proteins and modulating their activities by directly interacting with them [8]. It was already demonstrated that WA can induce apoptosis as well as autophagy in MCF-7 and MDA-MB-231 cells [9]. However, under similar conditions, cell death in the current study has shown features that are clearly distinct from typical apoptosis or autophagy. Therefore, further experimental evaluations with these cell lines were performed to better characterize programmed cell death under WA treatment.

Paraptosis is characterized by swelling of mitochondria and endoplasmic reticulum (ER), followed by creation of larger vacuoles due to their fusion. Some other features of paraptosis include absence of DNA fragmentation, chromatin condensation and PARP cleavage [10]. The appearance of swollen cells suggests ionic deregulation followed by water retention and ultimately disruption of intracellular ion homeostasis causing osmotic lysis, leading to cellular death [11]. Observations, that paraptosis can be inhibited by cycloheximide (CHX), indicate that the process requires protein synthesis [12], thereby distinguishing it from necrosis [4]. The first natural inhibitor of paraptosis, identified by Sperandio *et al.* [13], is known as AIP1/Alix, which is a protein cloned from a calcium-binding protein (ALG-2) involved in T-cell receptor induced cell death. Paraptosis can be activated by MAPK and JNK signaling pathways [13], the TNF receptor family member TAJ/TROY pathways [14] and the insulin-like growth factor I receptor pathways [10]. Paraptosis appears to be associated with the development of nervous system and neurodegeneration [15]. In addition, various stimuli, like curcumin [12] and ophiobolin-A [16] have been found to induce paraptosis-like cell death in apoptosis-resistant cancer cells. Compounds inhibiting proteasome activity in cancer cells may cause paraptosis-like cell death by inducing unfolded protein response (UPR) and, consequently, ER homeostasis disorder [17–19].

The potency of WA to induce paraptosis in cancer cells has been an untrodden mechanism. Our present study elucidates WA-induced oxidative stress mediated cell death in concert with certain specific characteristics of paraptosis in human breast cancer cell lines MCF-7 and MDA-MB-231.

## Materials and Methods

### Materials

WA was purchased from Alexis Biochemicals, USA. TritonX-100, FBS, DMEM, trypsin-EDTA solution, amphotericin B, penicillin and streptomycin were obtained from Hi-Media, Mumbai, India. DMSO, Wortmannin, Trypan blue, TMRE, Bradford reagent, Luminol,

Cycloheximide, Z-vad-fmk, H<sub>2</sub>DCFDA, NAC, P-formaldehyde, PI and HRP-conjugated anti-GAPDH antibody were from SIGMA-Aldrich, USA. Ascorbic acid was purchased from Merck, (Darmstadt, Germany). Cell lysis buffer was purchased from BD Pharmingen, USA. Annexin V-FITC apoptosis detection kit was from Cayman Chemicals, USA. Developer, fixer and X-ray films were from KODAK, Japan. Agar100 resin was obtained from Agar Scientific Co., UK. Trizol was purchased from Invitrogen (CA, USA). All reagents for RT-PCR were from Fermentas (Burlington, Canada). Other chemicals were of analytical grade and purchased locally.  $\beta$ -actin primary antibody and HRP conjugated anti-mouse, anti-rabbit secondary antibodies were obtained from Santacruz, USA. AIP1/Alix and PCNA antibodies were obtained from BioLegend, USA, GRP-78, CHOP antibodies from Cell-Signaling, USA.

## Methods

**Cell culture and treatments.** Human breast epithelial adeno-carcinoma cell-lines, MCF-7 and MDA-MB-231 were obtained from National Centre for Cell Science, Pune, India. All these cells were maintained in DMEM supplemented with 10% FBS, Amphotericin-B (1.25  $\mu$ g/ml), penicillin (100 IU/mL) and streptomycin (100  $\mu$ g/mL) at 37°C in a humidified atmosphere containing 5% CO<sub>2</sub>. Normal human breast epithelial cell line MCF-10A (a kind gift from Prof. P. K. Das, IICB) was used as a control cell line. MCF-10A was maintained in DMEM supplemented with 10% FBS, Amphotericin-B (1.25  $\mu$ g/ml), penicillin (100 IU/mL) and streptomycin (100  $\mu$ g/mL), horse serum (5%), Epidermal Growth Factor or EGF (20 ng/ml), hydrocortisone (0.5 mg/ml), cholera toxin (100 ng/ml), insulin (10  $\mu$ g/ml). Confluent cells (80%) were trypsinized, re-plated (2x10<sup>6</sup> cells) and allowed 18h for adhesion. Morphology of the cells was always observed under microscope (Olympus-CKX41). For treatment of MCF-10A cells, assay medium was used which contained all the supplements except EGF. Cells were treated with WA (4  $\mu$ M) for 24h or for desired time. Cells were also treated with WT (1  $\mu$ M) or z-VAD-fmk (25  $\mu$ M) or cycloheximide (2  $\mu$ M) or NAC (5mM) or ascorbic acid (100 $\mu$ M) for 24h or time as specified and with H<sub>2</sub>O<sub>2</sub> (10 mM) for 15 min in presence or absence of WA. Final DMSO concentrations were always maintained below 0.05% (v/v) where no anti-proliferative effects on cells were observed.

**Cell viability assay.** Following treatment with NAC (5mM) or CHX (2 $\mu$ M) in presence and absence of WA (4 $\mu$ M) for 24h, MCF-7, MDA-MB-231 and MCF-10A cells were collected in PBS (Phosphate buffered saline). Viable cells were counted by staining with trypan blue and  $\text{dIC}_{50}$  values were determined from three independent experiments [20].

**Measurement of Apoptosis, ROS and mitochondrial membrane potential ( $\Delta\psi$ m).** For detection of apoptosis, treated cells (2.5x10<sup>6</sup>) were washed with 1X PBS, stained doubly with FITC conjugated Annexin V antibody and PI (Propidium Iodide) according to manufacturer's instructions (Cayman Chemicals) and then subjected to flow-cytometric analysis [BD Fluorescence Activated Cell Sorter (ARIA II), San Jose, CA] using FACS Diva software.

Intracellular ROS generation was measured by changes in fluorescence intensity of H<sub>2</sub>DCFDA (excitation 480nm, emission 530 nm) by flow-cytometry using cells treated with H<sub>2</sub>DCFDA (10  $\mu$ M) in dark for 30 min at 37°C.

The changes in Mitochondrial Membrane Potential (MMP) of treated cells with respect to the controls (1x10<sup>6</sup>) were detected by exposing cells to different concentrations of WA or equal amount of DMSO (vehicle) for 24h, or 10 mM H<sub>2</sub>O<sub>2</sub> for 15 min, followed by incubating them with TMRE (100 nM) for 30 min at 37°C in dark. After washing with PBS, fluorescence intensities (PE-A, 575 nm) of 10,000 cells were analyzed by flow cytometry (BD FACS, ARIA II) using FACS Diva software.

**Western blot.** Total cell extracts were prepared from cells (2x10<sup>6</sup>) treated with WA (4  $\mu$ M) for 24h using lysis buffer (BD Pharmingen) according to manufacturer's instruction

and subjected to immunoblot as described previously [20]. Briefly, blots were incubated with primary antibodies (1:1000) against Alix, PCNA, GRP-78 and CHOP, followed by subsequent washing, and then addition of HRP conjugated secondary antibodies (1:5000). After thorough washing with TBS-T, bands were visualized by using Luminol reagents and exposing to X-ray film.  $\beta$ -actin was used as loading control.

**Transmission electron microscopy.** Following treatment; as specified in each case, cells were harvested, washed with PBS and fixed in ice-cold 2.5% glutaraldehyde in PBS, fixed in 1% osmium tetroxide, dehydrated through graded series of ethanol (30%–100%) and embedded in Agar100 resin. After ultrathin sections using an Ultracut ultramicrotome (Leica) and staining with uranyl acetate (saturated solution) and lead citrate (0.1%), samples were examined under FEI Tecnai 12BioTwin transmission electron microscope.

**Reverse-Transcription Polymerase Chain Reaction.** MCF-7 cells ( $3 \times 10^6$ ) were treated with 4  $\mu$ M of WA in presence and absence of antioxidant NAC (5mM) for 24h and total RNA was extracted using trizol (as manufacturer's instruction). 2  $\mu$ g of total RNA was reversed transcribed to prepare cDNA and PCR was performed with specific primers (XBP1: fwd: 5' - CCTTGTAGTTGAGAACCAGG-3'; rev: 5' - GGGGCTTGGTATATATGTGG-3' and 18S: fwd: 5' - TCAAGAACGAAAGTCGGAGG-3'; rev: 5' - GGACATCTAAGGGCATCAC-3') using GenAmp PCR system-9700 (Applied Biosystems) as described previously [21]. PCR Products were separated in 8% PAGE and after staining with EtBr (0.5%  $\mu$ g/ml), the bands were visualized by Gel Documentation (Bio-Rad).

**Statistical Analysis.** Data are presented as the mean  $\pm$  standard error (SE) of at least three independent experiments. Statistical analysis of data was conducted by using MS Excel.

## Results

### Extensive cytoplasmic vacuolation is the key feature of WA mediated cell death

Ultra-structural analysis of MCF-7 and MDA-MB-231 cells by Transmission Electron Microscope (TEM) demonstrated that treatment with WA for 24h induced extensive cytoplasmic vacuolation in both MCF-7 and MDA-MB-231 cells (Fig 1A).

### WA induced hyper-polarization of MMP (mitochondrial membrane potential)

TMRE is a cell permeable, positively-charged, red-orange fluorescent dye that readily accumulates in active mitochondria due to their relative negative charge and the uptake is directly proportional to the mitochondrial membrane potential ( $\Delta\psi_m$ ) of cells [22]. Depolarized or inactive mitochondria failed to sequester TMRE that indicate decreased membrane potential. Changes in MMP of MCF-7 and MDA-MB-231 cells treated with WA (0–8  $\mu$ M) were monitored by flow cytometry using TMRE. The intensities of TMRE fluorescence was continuously augmented by WA treatment for both the cell lines (Fig 1B) as compared to untreated (control), where treatment with  $H_2O_2$  showed depolarization of mitochondria. Increased MMP (mitochondrial hyperpolarization) could be indicative of substantial changes in mitochondrial metabolic activity and redox equilibria, which could finally lead to paraptosis.

### WA treatment is associated with morphological changes in mitochondria and Endoplasmic Reticulum

With respect to untreated controls, WA-treated (for 12h) cells displayed both enlarged mitochondria (Fig 1C) and Endoplasmic Reticulum (Fig 1D) as observed under TEM in MCF-7



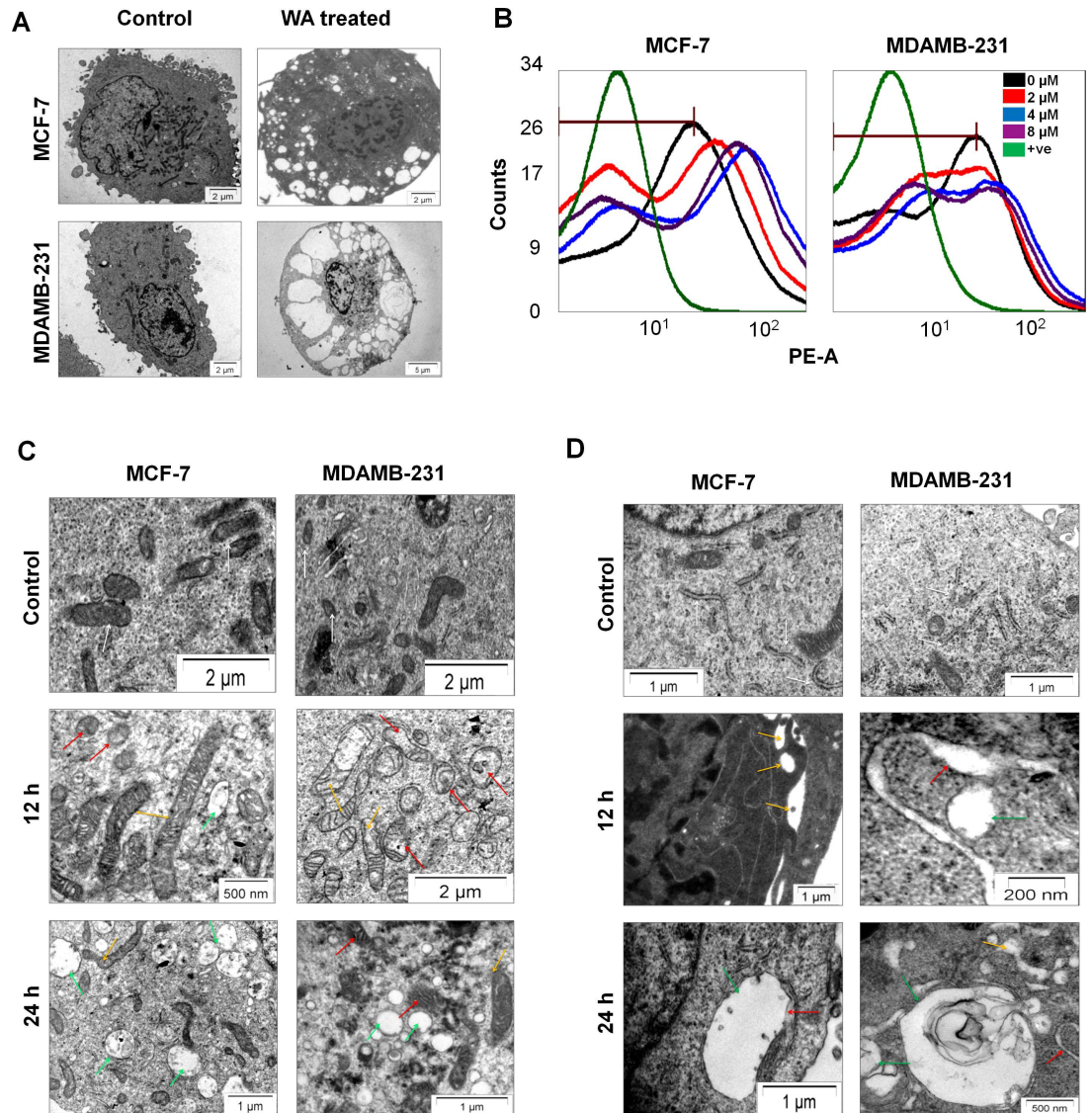


**Fig 1. WA induced cytoplasmic vacuolation and altered mitochondrial and ER homeostasis.** (A) Transmission electron micrographs of MCF-7 and MDA-MB-231 cells, treated with WA (4 $\mu$ M) for 24h showing the ultra-structural morphology of extensive cytoplasmic vacuolation. (B) MCF-7 and MDA-MB-231 cells were treated and stained with TMRE as described in method section. The graphs are representative of three individual identical experiments showing mitochondrial hyperpolarization by WA treatment, where “0  $\mu$ M” represents healthy control cells treated with equal amount of vehicle *i.e.* DMSO only for 24h, and “+ve” represents positive control *i.e.* cells treated with 10 mM H<sub>2</sub>O<sub>2</sub> for 15 mins for showing mitochondrial depolarization. Both MCF-7 and MDA-MB-231 cells were treated with 0–8  $\mu$ M of WA for 24h (sample were prepared as described in method section). Electron microscopic images showing the ultrastructural morphology of mitochondria (C); and ER (D); where white, red, yellow and green arrows indicate normal, swelled, enlarged (dilated) and vacuoles respectively.

doi:10.1371/journal.pone.0168488.g001

and MDA-MB-231 cells. Cellular mitochondria were found to be swollen and fused together forming mega-mitochondria (Fig 1C; yellow arrow) with dilated cristae (Fig 1C; red arrow), whereas healthy cells showed mitochondria with fine fibrous distributions (Fig 1C; white arrow). Due to WA treatment, size and number of the ER cisternae first got increased and then dilated (Fig 1D; yellow arrow). Subsequently, fusion among these dilated regions of ER contributed to large dilated empty vacuoles (Fig 1D; green arrow). Interestingly, at 24h post-

treatment, most of the ribosomes were found to be no longer appended to the ER membrane (Fig 1D; green arrow). Fusion of mitochondria and ER increased with time until the cells were almost fully occupied by mega-mitochondria and expanded vacuoles (Fig 1A, both MCF-7 and MDA-MB-231 cells). These observations all together resemble the pattern of paraptosis which is characterised by physical enlargement of both mitochondria and ER.

### Suppression of cellular endogenous protein Alix in WA induced cell death

When both MCF-7 and MDA-MB-231 cells were treated with 4 $\mu$ M WA for 24h, significant decrease in the expression of Alix, the known endogenous inhibitor of paraptosis [13] was evident (Fig 2A). Decreased expression of Alix/AIP-1 could be suggestive of induction of paraptosis by WA treatment in both the cell-lines.

### WA-induced cell death was interrupted by translation inhibitor

To check whether new protein synthesis is required for WA mediated cell death, both the breast cancer cell lines were treated for 24h with WA in presence or absence of cyclohexamide (CHX), a translational inhibitor, and cell viability was measured by trypan blue exclusion assay (Fig 2B). Results displayed that co-treatment with cyclohexamide inhibited WA-mediated cell death, indicating requirement of *de-novo* protein synthesis for cellular death that satisfy the necessary requirement for paraptosis.

Microscopic images of both MCF-7 and MDA-MB-231 cells (Fig 2C) shows extensive cytoplasmic vacuolation with morphological changes upon treatment with 4 $\mu$ M WA for 24h, as compared to respective control cells. These morphological changes and cellular death were abrogated by co-treatment with cyclohexamide, indicating vacuolation, morphological changes and cellular death to be associated with *de-novo* protein synthesis.

### Autophagy inhibitor has no effect on WA-induced cytoplasmic vacuolation

To distinguish between WA-induced intracellular vacuolation and autophagic cell death, MCF-7 and MDA-MB-231 cells were treated with WA (4  $\mu$ M) in presence and absence of autophagy inhibitor, WT (1  $\mu$ M) and observed under TEM. Most strikingly, WT was merely found to prevent the formation of WA-induced gigantic perinuclear vacuoles (Fig 3A), which established that autophagy is not entirely responsible for WA-induced cytoplasmic vacuolation for the cell-lines under investigation.

### Sensitivity of human breast cancer cells to WA in presence and absence of pan-caspase inhibitor

To assess the involvement of caspases in WA-induced cell death, MCF-7 and MDA-MB-231 cells were pre-treated with a pan-inhibitor of caspases (z-VAD-fmk) followed by treatment with WA (4  $\mu$ M) for 24h and the amount of cell death was measured by FACS using annexin/PI double staining method. In the case of MCF-7 cells, 36.8 $\pm$ 2.8% cells were found to be necrotic with negligible population of apoptotic cells (Fig 3B), which firmly suggested that apoptosis is not the major mode of WA-mediated cell death in MCF-7 cells. However, in the case of MDA-MB-231 cells, the apoptotic and necrotic populations were 36.6 $\pm$ 0.02% and 17.7 $\pm$ 3.1% respectively, signifying the fact that MDA-MB-231 cells undergo significant apoptosis on WA treatment. Co-treatment with WA and z-VAD-fmk increased the necrotic population significantly (from 36.8 $\pm$ 2.8% to 66.7 $\pm$ 1.8%) in MCF-7 cells with no change in the apoptotic

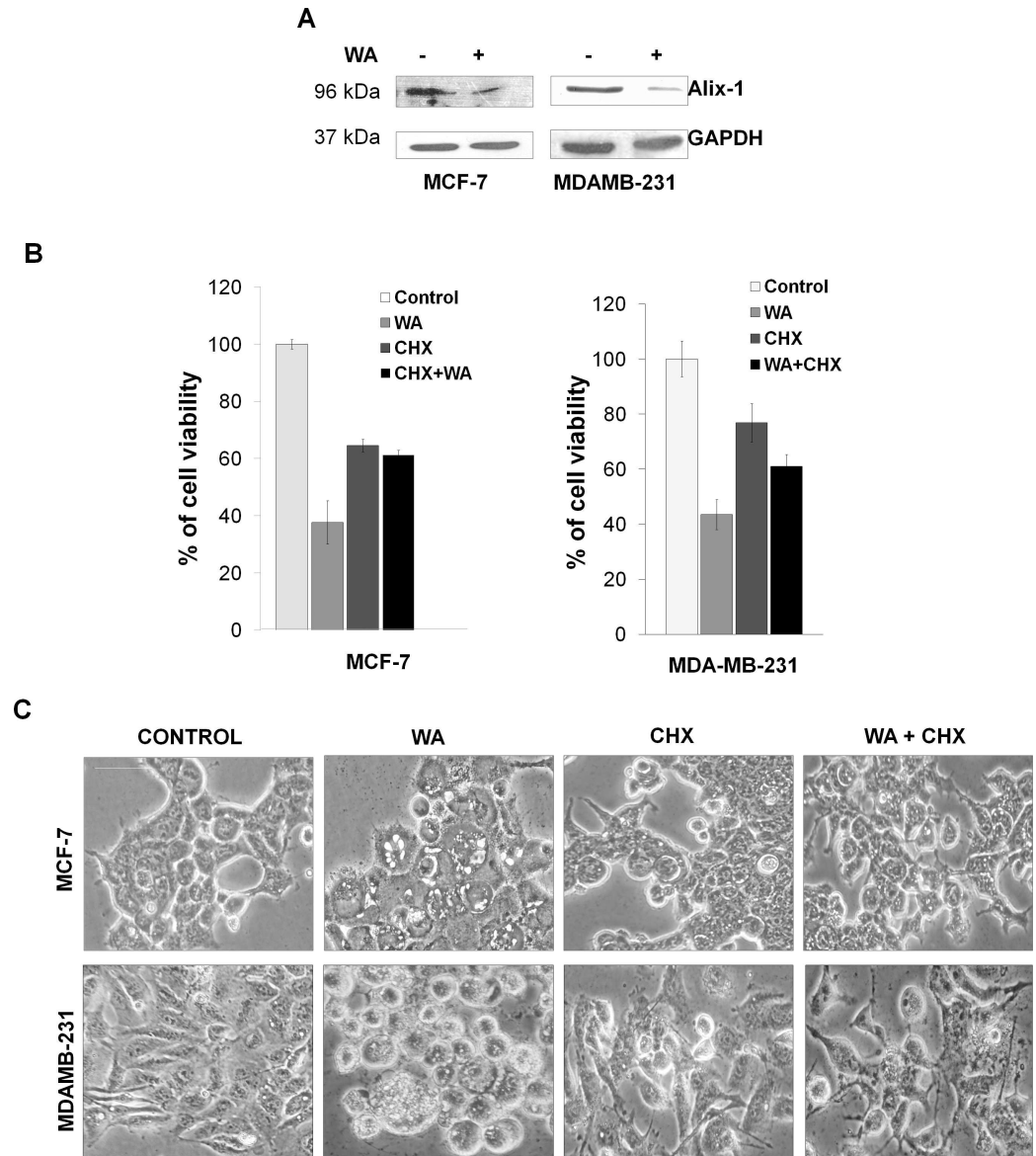


**Fig 2. WA induced paraptosis in cells.** (A) Representative western blot from three separate experiments for Alix-1 protein using cell lysates of MCF-7 and MDA-MB-231 cells treated or untreated with 4  $\mu$ M WA for 24h, where GAPDH used as loading control. (B) MCF-7 and MDA-MB-231 cells were treated with/without 4  $\mu$ M of WA for 24h in presence and absence of CHX (2  $\mu$ M) and cell growth inhibition was assessed by Trypan blue exclusion assay. Percentage of viable cells were plotted against drug treatment, where the columns are the mean of three independent determinations; bars, standard error (SEM); ( $P < 0.05$  corresponding to control,  $n = 3$ ). (C) Phase contrast images of MCF-7 and MDA-MB-231 cells, treated with either DMSO or 4  $\mu$ M of WA for 24h in presence and absence of CHX. Scale bars represent 50  $\mu$ m and images are representative of at least three independent experiments.

doi:10.1371/journal.pone.0168488.g002

population, whereas, in MDA-MB-231 cells, co-treatment decreased the apoptotic population (from  $36.6 \pm 0.02\%$  to  $1.95 \pm 0.63\%$ ) with concomitant increase in the necrotic population (from  $17.7 \pm 3.1\%$  to  $38.6 \pm 1.5\%$ ) as compared to cells treated with WA alone. These results indicate that WA induced apoptosis in MDA-MB-231 cells, which was inhibited by addition of caspase inhibitor and the cells underwent caspase-independent cell death. On co-treatment with WA and z-VAD-fmk, increase in cell death (from  $39.7 \pm 1.9\%$  to  $67.6 \pm 2.3\%$ ) in MCF-7



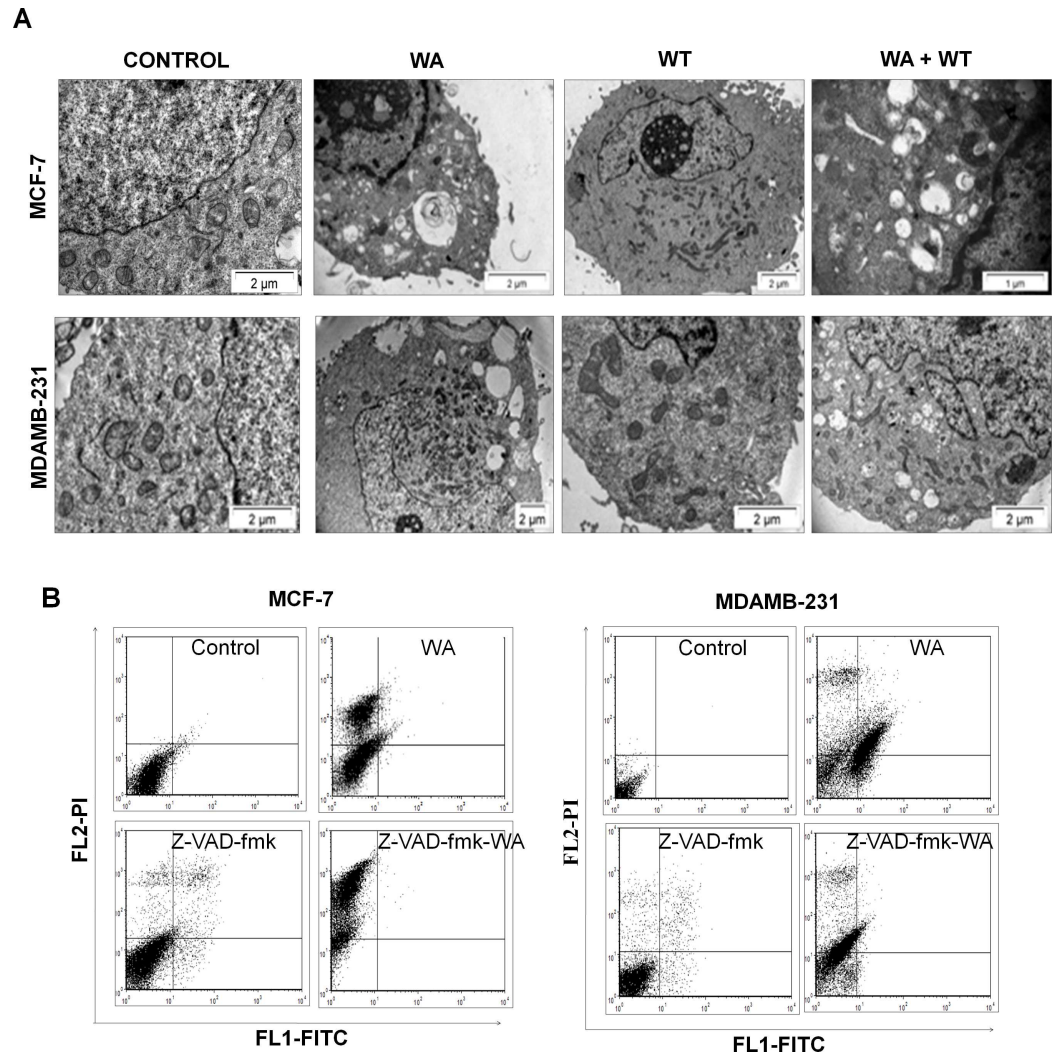


**Fig 3. Effect of autophagy and apoptosis inhibitors on WA mediated cell death.** (A) Transmission electron micrographs of MCF-7 and MDA-MB-231 cells, treated with either DMSO or WA (4  $\mu$ M) in presence and absence of autophagy inhibitor WT for 24h. (B) For apoptosis assay both MCF-7 and MDA-MB-231 cells were either treated with DMSO, WA (4  $\mu$ M) or pre-treated with zVAD-fmk in presence or absence of WA (4  $\mu$ M). Cells were harvested after 24h exposure and stained with annexin V-FITC and PI. The samples were analysed using flow cytometer. The percentage of earlyapoptotic, late apoptotic and necrotic cells was located in the lower right (annexin V-FITC positive/PI negative cells), upper right (annexin V-FITC positive/PI positive cells) and upper left (PI positive cells) quadrant respectively.

doi:10.1371/journal.pone.0168488.g003

cells in contrast with partial decrease in total cell death (from  $57.5 \pm 3.2\%$  to  $38.4 \pm 2.1\%$ ) in MDA-MB-231 cells was clearly evident (refer to left panel of [S1 Fig](#)). In conclusion, WA induced death in MDA-MB-231 cells is through both apoptosis and caspase-independent mode; in contrast, death was found to be entirely non-apoptotic and caspase independent in MCF-7 cells.

### WA induced death in breast cancer cells are mediated by ROS pathway

WA was found to trigger an early induction of ROS, 1.5h and 3h post treatment for MCF-7 and MDA-MB-231 cells respectively, which gradually decreased over time ([Fig 4A](#)). However, no such increase in ROS generation was observed for WA treatment of normal control breast cancer cell line MCF-10A (top left panel of [S2 Fig](#)).



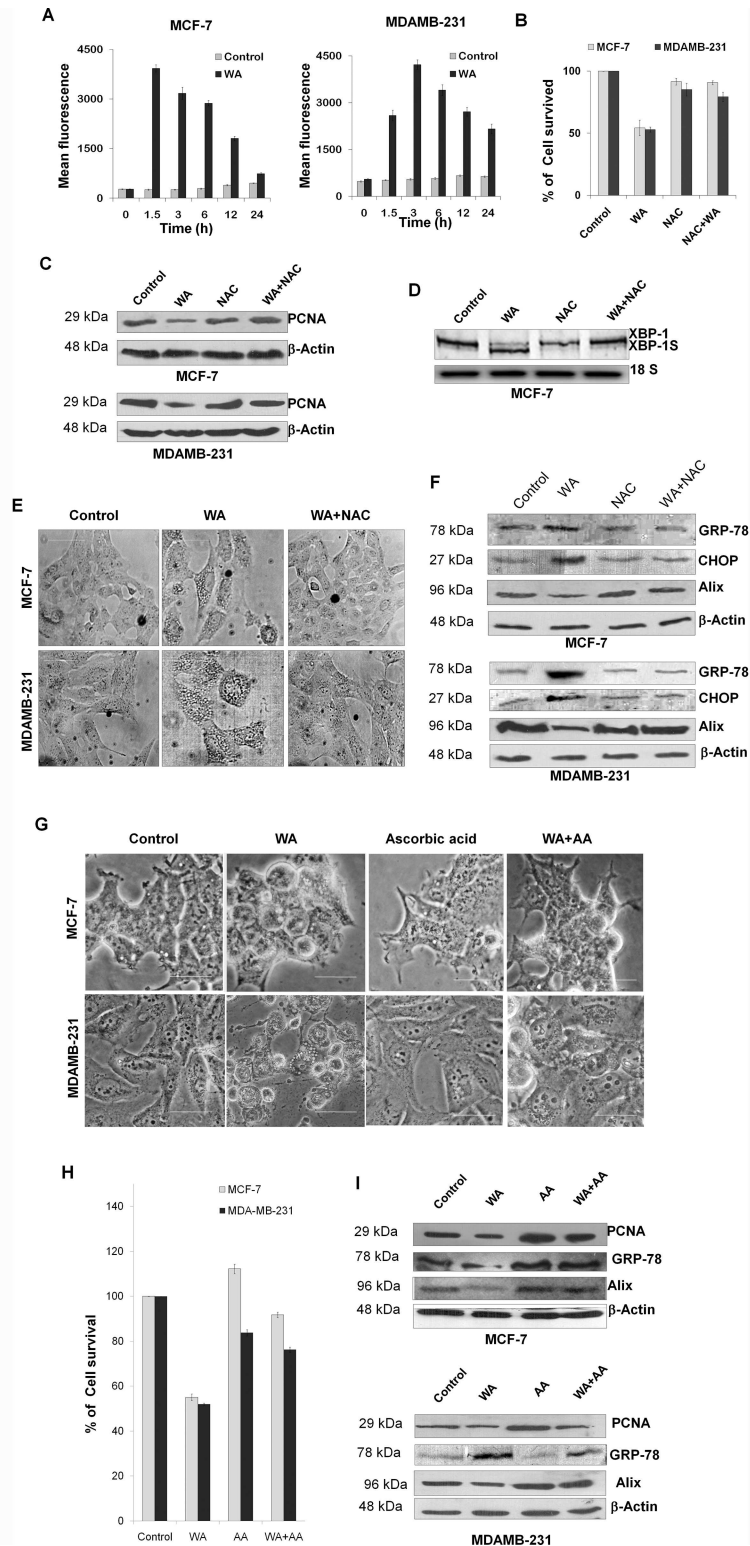


**Fig 4. Effect of WA intrinsic ROS generation, ROS mediated ER-stress and paraptosis. (A)** The inter-cellular ROS generation in WA-treated MCF-7 and MDA-MB-231 cells was measured flow cytometrically by the intensity of H<sub>2</sub>-DCFDA fluorescence. Bar diagram showing mean fluorescence intensity plotted against different time intervals where each point represents as the mean ± SEM of triplicate experiments (P < 0.05 corresponding to control, n = 3). **(B)** Cell growth inhibition of MCF-7 and MDA-MB-231 cells treated with/without WA (4 μM) for 24h in presence and

absence of NAC (ROS scavenger) was assessed by Trypan blue exclusion assay. Percentage of viable cells were plotted against drug concentrations, where the columns are the mean of three independent determinations; bars, standard error (SEM); ( $P < 0.05$  corresponding to control,  $n = 3$ ). (C) Representative western blot from three separate experiments for PCNA protein using cell lysates of MCF-7 and MDA-MB-231 cells treated with/without WA (4  $\mu\text{M}$ ) for 24h in presence and absence of NAC, where  $\beta$ -actin was used as loading control. (D) Total RNA was extracted from MCF-7 cells (treated with/without 4  $\mu\text{M}$  of WA for 24h in presence and absence of NAC) and subjected to RT-PCR where unspliced (XBP1) and spliced (XBP-1s) form of XBP-1 mRNA expression was shown. 18S rRNA was used as loading control. (E) Phase contrast images MCF-7 and MDA-MB-231 cells treated (24h) with DMSO or WA (4  $\mu\text{M}$ ) in presence or absence of NAC. Scale bars represent 50 micron and images are representative of at least three independent experiments. (F) Immune reactive bands of proteins GRP-78, CHOP and Alix extracted from MCF-7 and MDA-MB-231 cells treated with/without 4  $\mu\text{M}$  of WA for 24h in presence and absence of NAC where GAPDH was used as loading controls. (G) Phase contrast images of MCF-7 and MDA-MB-231 cells, treated with either 0 or 4  $\mu\text{M}$  of WA for 24h in presence and absence of ascorbic acid (100  $\mu\text{M}$ ). Scale bars represent 50  $\mu\text{m}$ . (H) Cell growth inhibition of MCF-7 and MDA-MB-231 cells treated with/without WA (4  $\mu\text{M}$ ) for 24h in presence and absence of ascorbic acid (another ROS scavenger) was assessed by Trypan blue exclusion assay. Percentage of viable cells were plotted against drug concentrations, where the columns are the mean of three independent determinations; bars, standard error (SEM). (I) Western blots from three separate experiments for PCNA, Alix and GRP-78 proteins using cell lysates of MCF-7 and MDA-MB-231 cells treated with/without WA (4  $\mu\text{M}$ ) for 24h in presence and absence of ascorbic acid, where  $\beta$ -actin was used as loading control.

doi:10.1371/journal.pone.0168488.g004

Treatment with NAC (5mM), an inhibitor of ROS generation, predominantly inhibited WA-mediated cellular death in MCF-7 and MDA-MB-231 cells (Fig 4B), whereas no significant effect was found in control MCF-10A cells (top right panel of S2 Fig). Down regulation of the level of a proliferation associated protein, PCNA (Fig 4C) was observed for both MCF-7 and MDA-MB-231 *w.r.t.* WA treated cells. PCNA is a proliferative marker, so this result suggests that an early onset of ROS induction was required for WA mediated death or inhibition of proliferation in both the cells.

ROS activates numerous signaling pathways and perform important functions in cells [12]. However, excessive ROS production can induce ER stress-mediated unfolded protein response. Thus, to determine whether WA induced ROS has any role in the induction of UPR in breast cancer cells; cellular RNA was extracted and used for RT-PCR to monitor splicing of XBP-1 mRNA. As shown in Fig 4D, the spliced form of XBP-1 mRNA (*i.e.* XBP-1s) was clearly detectable in cells treated with only WA, however this splicing of XBP-1 was found to be abrogated in presence of NAC compared to its respective control.

Further, it was observed under phase contrast microscope that treatment with WA for 12h induced extensive cytoplasmic vacuolation (Fig 4E), which was abrogated by co-treatment with NAC indicating WA-induced early onset of redox imbalance could be responsible for the changes associated with induction of extensive cytoplasmic vacuolation. However, in the case of control MCF-10A cells, no significant vacuolation was observed on WA treatment (Left bottom of S2 Fig).

As shown in Fig 4F, for MCF-7 and MDA-MB-231 cells respectively, the expression levels of ER-stress related proteins like GRP-78 (Bip) and CHOP showed marked elevation by WA treatment which got reduced in presence of NAC, whereas, MCF-10A showed no significant overexpression of GRP-78 (right bottom panel of S2 Fig). Furthermore, a significant decrease in the expression of Alix/AIP-1 was found on WA treatment, which was suppressed by co-treatment with NAC, suggestive of the fact that induction of ER-stress by WA is happening through ROS mediated pathway, leading to paraptosis mediated cellular death in both the breast cancer cell-lines.

To rule out the possibility that NAC could be involved in covalent interactions with WA [8], both the cells were treated with another ROS inhibitor, ascorbic acid (100  $\mu\text{M}$ ) [23] for 6h, followed by WA treatment and checked cytoplasmic vacuolation, percentage of cell survival and the levels of proliferation associated factor and ER-stress related factors. Phase contrast microscopic images (Fig 4G) showed that treatment with WA for 24 h induced extensive

cytoplasmic vacuolation, which was abrogated by co-treatment with ascorbic acid, that corresponds to the earlier observations using NAC. Treatment with ascorbic acid also predominantly inhibited WA-mediated cellular death (Fig 4H), down regulation of PCNA and Alix, along with marked elevation of ER-stress related protein GRP-78 (Bip) (Fig 4I). Thus, similar results on treatment with both ROS inhibitors suggest that paraptosis is mediated through early ROS induction by WA in MCF-7 and MDA-MB-231 cells.

## Discussion

Paraptosis is a novel kind of 'Programmed Cell Death' (PCD) pathway found to be morphologically and biochemically distinct from apoptosis. This kind of non-apoptotic cell death has been discovered recently and thus its molecular mechanisms have not been fully documented yet. For the last few years, several reports indicated WA as a potent inducer of apoptosis in diverse human carcinomas [8], but as per our knowledge, no report yet published has presented the involvement of WA in paraptotic cell death in any human cancer. Here, we have established for the first time that WA has the capability to induce paraptosis, a non-apoptotic alternative form of PCD in human breast cancer cell-lines.

Apparently, WA elicits extensive cytoplasmic vacuolization in both the cells. Characterization of these WA induced cytoplasmic vacuolization indicated that, it was mostly generated from stress mediated dilation of ER cisternae or swelling and enlargement of mitochondria that bear close resemblance with typical characteristics of paraptosis [10, 13, 14]. Furthermore, cycloheximide (inhibitor of translation) dramatically suppressed the toxicity exerted by WA implying that WA mediated morphological changes and cellular death required *de novo* synthesis of protein [12]. And finally the negative involvement of AIP-1/Alix [13] (endogenous paraptosis inhibitor) protein suggested that WA-induced cell death in case of both MCF-7 and MDA-MB-231 cells is certainly related to paraptosis.

Paraptosis sometimes shows resemblance to necrosis since these two modes of cell death mechanism share some similar kind of morphological features like vacuolization and mitochondrial swelling, along with lack of activation of caspases [10]. It is well known that *in vitro* cell death by caspase dependent apoptosis often results in secondary necrosis [10]. In the present study, the role of caspase activation cannot be ruled out totally since z-VAD-fmk was found to increase the PI-positive population significantly in both the cells which could be necrosis. However, when the cells were visualized under TEM, the paraptotic characteristics were evident in both the cells as early as 12h after exposure to WA, long before any dead cells appeared. These results clearly suggested that most of the PI-positive MCF-7 and MDA-MB-231 cells that resulted from WA exposure were committed to paraptosis and not necrosis. In the case of MCF-7 cells no distinctive characteristics of apoptosis, like DNA ladder formation or nuclear condensation and blebbing were observed (refer S3 Fig). However, unlike MCF-7 cells, in MDA-MB-231 cells WA induced apoptosis along with paraptosis. Interestingly it was found that WA-induced vacuolization and cell death in human breast cancer cell-lines were not affected by autophagy inhibitor, wortmannin, excluding the possibility of autophagy-mediated cell death.

Transmission electron micrographs of WA treated cells revealed severe alteration in mitochondrial morphology (both internal structural features and external shape) implying that mitochondrial swelling could be deemed as a WA induced paraptosis hallmark. MMP depletion generally precedes apoptotic cell death [24]. However, recent studies revealed a key role of mitochondrial permeability transition also in necrosis and mitotic catastrophe [25]. Strikingly, WA-induced mitochondrial swelling displayed hyperpolarization of MMP instead of depletion of mitochondrial membrane potential (MMP), suggesting a significant correlation with substantial changes in mitochondrial metabolic homeostasis as well as ionic imbalance as reported

earlier [26]. The ER plays an important role in the processing, folding and export of newly synthesized proteins to the secretory pathway. It has been found that failure of proteasomal degradation system leads to accumulation of misfolded proteins in the ER and cytoplasm. This eventually overwhelms cells and induces ER stress-mediated UPR to protect cells from proteotoxicity [19] but insurmountable disturbance of ER homeostasis may also lead to paraptosis-like cellular death. In a different study, we have found that WA inhibits ubiquitin-mediated proteasomal system and as a consequence, accumulates ubiquitinated proteins over time in case of MCF-7 and MDA-MB-231 cells (unpublished data, not shown here).

Morphological analysis of WA treated cells under TEM revealed that a time-dependent formation of cytoplasmic vacuoles probably derived from ER swelling. At the same time, it also showed dissociation of ribosomes from ER membrane, indicating manifestation of ER-stress mediated UPR that eventually stops new protein synthesis to relieve ER stress [27]. These observations were further paralleled by the levels of XBP-1 spliced mRNA in WA treated cells confirming the concomitant induction of the UPR [28]. Consequently, WA was also found to accumulate ER chaperon proteins in human breast cancer cells (unpublished data; not shown here).

It is worth noting that WA induced paraptosis was associated with a huge induction of oxidative stress in early hours (1.5h-3h) of WA treatment in cells, followed by gradual decrease over time. ROS constitute a crucial group of molecules that mediate numerous signal transduction pathways and perform critical functions in cells [12]. Most cancer cells exhibit increased aerobic glycolysis and oxidative stress compared to those of their normal counterparts [12]. However, an increase in ROS production past a certain level can interfere with ER function, causing the accumulation of large amounts of unfolded or misfolded proteins and leading to the cellular ER stress response [29]. Since WA-mediated formation of cytoplasmic vacuoles, splicing of XBP-1 mRNA, expression of ER-stress related proteins like GRP78 and CHOP and cellular death were found to be abrogated by co-treatment of cells with the antioxidant NAC as well as ascorbic acid, it could be logical to assume that WA induced paraptotic changes in cells were downstream of the WA mediated ROS generation. Thus, WA induced ER stress could be intimately intertwined with its ability to alter cellular redox balance; however further experimental evidence are required to clarify how WA induced oxidative imbalance influence ER homeostasis which in turn resulted in paraptotic cell death in these human breast cancer cell lines.

Apoptosis resistance is a major obstacle to successful chemotherapy in patients with advanced breast carcinoma and is correlated with the metastatic potential of tumor cells [30]. Conquering this issue is a key goal to re-sensitize tumor cells to cancer therapy by targeting differential mode of programmed cell death pathway(s) [5]. Our results indicated that; in human breast cancer cell-lines MCF-7 and MDA-MB-231, WA induces a novel cytoplasmic vacuolation-mediated cell death (paraptosis), which is distinct from the apoptotic and autophagic cell death pathways. This novel pathway may prevent cancer cells from developing apoptosis or autophagy resistance after the completion of drug treatment. To further understand its mechanisms, we revealed that WA-induced ROS release is an initial signal for the perturbation of ER homeostasis, which subsequently induced cytoplasmic vacuolation mediated cell death. Further investigation of the molecular mechanisms underlying WA-induced paraptosis may lead to the development of a novel therapeutic approach for the more effective management of breast cancer cells undergoing death through similar pathways.

## Supporting Information

**S1 Fig. Effect of caspase inhibitor Z-VAD-fmk on apoptotic cell death in MCF-7 and MDA-MB-231 cells.** Apoptotic cell death in WA treated cells by annexin V-FITC/PI double



staining method. For apoptosis assay both MCF-7 and MDAMB-231 cells were either treated with DMSO, WA (4  $\mu$ M) or pre-treated with zVAD-fmk in presence or absence of WA (4  $\mu$ M). Cells were harvested after 24h exposure and stained with annexin V-FITC and PI. The samples were analysed using flow cytometer. The percentage of total cell death (late apoptotic + necrotic population) was plotted against drug treatments. Each point represented as the mean  $\pm$  SEM of triplicate experiments ( $P < 0.05$  corresponding to control,  $n = 3$ ). (TIF)

**S2 Fig. Study of ROS generation, cell viability, cellular morphology and expression of ER stress related protein, GRP-78 in control MCF-10A cells.** (Top left panel) Graph (representative of three individual identical experiments) showing ROS generation by WA treatment in case of MCF-10A cells. Here “DMSO (control)” represents healthy cells treated with equal amount of vehicle i.e. DMSO for 6h, and “positive control” represents cells treated with 10 mM H<sub>2</sub>O<sub>2</sub> for 15 mins, otherwise cells were treated with 4  $\mu$ M of WA for different time periods (as mentioned in the figure). Cells were treated with H<sub>2</sub>DCFDA (10  $\mu$ M) in dark for 30 min at 37°C and intracellular ROS generation was measured by changes in fluorescence intensity of H<sub>2</sub>DCFDA (excitation 480 nm, emission 530 nm) by flow-cytometry. (Top right panel) Cell growth inhibition of MCF-10A cells treated with/without WA (4  $\mu$ M) for 24h in presence and absence of NAC (ROS scavenger) was assessed by Trypan blue exclusion assay. Percentage of viable cells were plotted against drug concentrations, where the columns are the mean of three independent determinations; bars, standard error (SEM). (Left bottom panel) Phase contrast images of MCF-10A cells, treated with either 0 or 4  $\mu$ M of WA for 24h in presence and absence of NAC. Scale bars represent 50  $\mu$ m. (Right bottom panel) Western blot showing expression of GRP-78 of control and WA-treated MCF-10A cells (whole cell extract). (TIF)

**S3 Fig. Study of apoptosis in MCF-7 cells by nucleosomal DNA fragmentation and DAPI staining of nuclei on WA treatment.** (Left panel) Nucleosomal DNA fragmentation in WA treated MCF-7 cells. Cultured MCF-7 cells were treated with different concentrations of (0–8  $\mu$ M) WA for 24h. DNA was isolated from each samples and subjected to agarose gel electrophoresis, and visualized by EtBr staining. (Right panel) MCF-7 cells were grown on glass coverslips and were exposed to DMSO or 4  $\mu$ M of WA for 24h, followed by fixing permeabilized and morphology of nuclei were visualized with an Olympus model CKX41 inverted microscope after staining with DAPI (1  $\mu$ g/mL) for 30 min in dark. (TIF)

## Acknowledgments

The authors wish to thank Dr. Mamta Chawla Sarkar and Mr. Gorge Banik (NICED) for allowing us to use their Flowcytometer, Prof. A.N. Ghosh (NICED) for enabling us to acquire Transmission Electron Microscopic images of samples.

## Author Contributions

**Conceptualization:** KG SS(B).

**Data curation:** KG S. De S. Das SM.

**Funding acquisition:** SS(B).

**Investigation:** KG S. De S. Das SM SS(B).

**Methodology:** KG S. De S. Das SM.

**Project administration:** SS(B).

**Software:** KG S. Das SM.

**Supervision:** SS(B).

**Validation:** KG S. De S. Das SM SS(B).

**Visualization:** KG SS(B).

**Writing – original draft:** KG SS(B).

**Writing – review & editing:** KG SM SS(B).

## References

1. Elmore S. Apoptosis: a review of programmed cell death. *Toxicol Pathol.* 2007; 35(4): 495–516. doi: [10.1080/01926230701320337](https://doi.org/10.1080/01926230701320337) PMID: [17562483](https://pubmed.ncbi.nlm.nih.gov/17562483/)
2. Brown JM, Attardi LD. The role of apoptosis in cancer development and treatment response. *Nat Rev Cancer.* 2005; 5(3): 231–237. doi: [10.1038/nrc1560](https://doi.org/10.1038/nrc1560) PMID: [15738985](https://pubmed.ncbi.nlm.nih.gov/15738985/)
3. Tsujimoto Y, Shimizu S. Another way to die: autophagic programmed cell death. *Cell Death Differ.* 2005; 12: 1528–1534. doi: [10.1038/sj.cdd.4401777](https://doi.org/10.1038/sj.cdd.4401777) PMID: [16247500](https://pubmed.ncbi.nlm.nih.gov/16247500/)
4. Clarke PG. Developmental cell death: morphological diversity and multiple mechanisms. *Anat Embryol (Berl).* 1990; 181(3): 195–213.
5. Okada H, Mak TW. Pathways of apoptotic and non-apoptotic death in tumour cells. *Nat Rev Cancer.* 2004; 4(8):592–603. doi: [10.1038/nrc1412](https://doi.org/10.1038/nrc1412) PMID: [15286739](https://pubmed.ncbi.nlm.nih.gov/15286739/)
6. Kitanaka C, Kuchino Y. Caspase-independent programmed cell death with necrotic morphology. *Cell Death Differ.* 1999; 6(6): 508–515. doi: [10.1038/sj.cdd.4400526](https://doi.org/10.1038/sj.cdd.4400526) PMID: [10381653](https://pubmed.ncbi.nlm.nih.gov/10381653/)
7. Nikolettou V, Markaki M, Palikaras K, Tavernarakis N. Crosstalk between apoptosis, necrosis and autophagy. *Biochim Biophys Acta.* 2013; 1833(12): 3448–3459. doi: [10.1016/j.bbamcr.2013.06.001](https://doi.org/10.1016/j.bbamcr.2013.06.001) PMID: [23770045](https://pubmed.ncbi.nlm.nih.gov/23770045/)
8. Vanden Berghe W, Sabbe L, Kaileh M, Haegeman G, Heyninck K. Molecular insight in the multifunctional activities of Withaferin A. *Biochem Pharmacol.* 2012; 84(10): 1282–1291. doi: [10.1016/j.bcp.2012.08.027](https://doi.org/10.1016/j.bcp.2012.08.027) PMID: [22981382](https://pubmed.ncbi.nlm.nih.gov/22981382/)
9. Hahm ER, Singh SV. Autophagy fails to alter Withaferin A-mediated lethality in human breast cancer cell lines. *Curr Cancer Drug Targets.* 2013; 13(6):640–650. PMID: [23607597](https://pubmed.ncbi.nlm.nih.gov/23607597/)
10. Sperandio S, De Belle I, Bredesen DE. An alternative, non-apoptotic form of programmed cell death. *Proc Natl Acad Sci USA.* 2000; 97(26):14376–14381. doi: [10.1073/pnas.97.26.14376](https://doi.org/10.1073/pnas.97.26.14376) PMID: [11121041](https://pubmed.ncbi.nlm.nih.gov/11121041/)
11. Hoa N, Myers MP, Douglass TG, et al. Molecular Mechanisms of Paraptosis Induction: Implications for a Non-Genetically Modified Tumor Vaccine. Pockley G, ed. *PLoS ONE.* 2009; 4 (2):e4631. doi: [10.1371/journal.pone.0004631](https://doi.org/10.1371/journal.pone.0004631) PMID: [19247476](https://pubmed.ncbi.nlm.nih.gov/19247476/)
12. Yoon MJ, Kim EH, Lim JH, Kwon TK, Choi KS. Superoxide anion and proteasomal dysfunction contribute to curcumin-induced paraptosis of malignant breast cancer cells. *Free Radic Biol Med.* 2010; 48 (5):713–726. doi: [10.1016/j.freeradbiomed.2009.12.016](https://doi.org/10.1016/j.freeradbiomed.2009.12.016) PMID: [20036734](https://pubmed.ncbi.nlm.nih.gov/20036734/)
13. Sperandio S, Poksay K, de Belle I, Lafuente MJ, Liu B, Nasir J, Bredesen DE. Paraptosis: mediation by MAP kinases and inhibition by AIP-1/Alix. *Cell Death Differ.* 2004; 11(10): 1066–1075. doi: [10.1038/sj.cdd.4401465](https://doi.org/10.1038/sj.cdd.4401465) PMID: [15195070](https://pubmed.ncbi.nlm.nih.gov/15195070/)
14. Wang Y, Lin N, Wang L, Ding P, Zhang D, Han W, Ma D. An alternative form of paraptosis-like cell death triggered by TAJ/TROY and enhanced by PDCD5 overexpression. *J Cell Sci.* 2004; 117:1525–1532. doi: [10.1242/jcs.00994](https://doi.org/10.1242/jcs.00994) PMID: [15020679](https://pubmed.ncbi.nlm.nih.gov/15020679/)
15. Turmaine M, Raza A, Mahal A, Mangiarini L, Bates GP, Davies SW. Non-apoptotic neurodegeneration in a transgenic mouse model of Huntington's disease. *Proc Natl Acad Sci USA.* 2000; 97(14):8093–8097. doi: [10.1073/pnas.110078997](https://doi.org/10.1073/pnas.110078997) PMID: [10869421](https://pubmed.ncbi.nlm.nih.gov/10869421/)
16. Bury M, Girault A, Megalizzi V, Spiegl-Kreinecker S, Mathieu V, Berger W et al. Ophiobolin-A induces paraptosis-like cell death in human glioblastoma cells by decreasing BKCa channel activity. *Cell Death Dis.* 2013; 4: e561. doi: [10.1038/cddis.2013.85](https://doi.org/10.1038/cddis.2013.85) PMID: [23538442](https://pubmed.ncbi.nlm.nih.gov/23538442/)
17. Yoon MJ, Kang YJ, Lee JA, Kim IY, Kim MA, Lee YS et al. Stronger proteasomal inhibition and higher CHOP induction are responsible for more effective induction of paraptosis by dimethoxy curcumin than curcumin. *Cell Death Dis.* 2014; 5: e1112. doi: [10.1038/cddis.2014.85](https://doi.org/10.1038/cddis.2014.85) PMID: [24625971](https://pubmed.ncbi.nlm.nih.gov/24625971/)

18. Gandin V, Pellei M, Tisato F, Porchia M, Santini C, Marzano C. A novel copper complex induces paraptosis in colon cancer cells via the activation of ER stress signalling. *J Cell Mol Med.* 2012; 16(1): 142–151. doi: [10.1111/j.1582-4934.2011.01292.x](https://doi.org/10.1111/j.1582-4934.2011.01292.x) PMID: [21388518](https://pubmed.ncbi.nlm.nih.gov/21388518/)
19. Tardito S, Isella C, Medico E, Marchiò L, Bevilacqua E, Hatzoglou M, Bussolati O, Franchi-Gazzola R. The thioxotriazole copper(II) complex A0 induces endoplasmic reticulum stress and paraptotic death in human cancer cells. *J Biol Chem.* 2009; 284(36):24306–24319. doi: [10.1074/jbc.M109.026583](https://doi.org/10.1074/jbc.M109.026583) PMID: [19561079](https://pubmed.ncbi.nlm.nih.gov/19561079/)
20. Dasgupta P, Bandyopadhyay SS. Role of di-allyldisulfide, a garlic component in NFκB mediated transient G2-M phase arrest and apoptosis in human leukemic cell-lines. *Nutr Cancer.* 2013; 65(4):611–622. doi: [10.1080/01635581.2013.776090](https://doi.org/10.1080/01635581.2013.776090) PMID: [23659453](https://pubmed.ncbi.nlm.nih.gov/23659453/)
21. Saha S, Chakraborty A, Bandyopadhyay SS. Stabilization of oncostatin-M mRNA by binding of nucleolin to a GC-rich element in its 3'-UTR. *J Cell Biochem.* 2016; 117(4): 988–999. doi: [10.1002/jcb.25384](https://doi.org/10.1002/jcb.25384) PMID: [26399567](https://pubmed.ncbi.nlm.nih.gov/26399567/)
22. Scaduto RC Jr, Grotzmann LW. Measurement of mitochondrial membrane potential using fluorescent rhodamine derivatives. *Biophys J.* 1999; 76: 469–477. doi: [10.1016/S0006-3495\(99\)77214-0](https://doi.org/10.1016/S0006-3495(99)77214-0) PMID: [9876159](https://pubmed.ncbi.nlm.nih.gov/9876159/)
23. Tor YS, Yazan LS, Foo JB, Wibowo A, Ismail N, Cheah YK, et al. (2015) Induction of Apoptosis in MCF-7 Cells via Oxidative Stress Generation, Mitochondria-Dependent and Caspase-Independent Pathway by Ethyl Acetate Extract of *Dillenia suffruticosa* and Its Chemical Profile. *PLoS ONE* 10(6): e0127441. doi: [10.1371/journal.pone.0127441](https://doi.org/10.1371/journal.pone.0127441) PMID: [26047480](https://pubmed.ncbi.nlm.nih.gov/26047480/)
24. Wyllie AH, Kerr JFR, Currie AR. Cell death: the significance of apoptosis. *Int Rev Cytol.* 1980; 68:251–306. PMID: [7014501](https://pubmed.ncbi.nlm.nih.gov/7014501/)
25. Zamzami N, Larochette N, Kroemer G. Mitochondrial permeability transition in apoptosis and necrosis. *Cell Death Differ.* 2005; 12:1478–1480. doi: [10.1038/sj.cdd.4401682](https://doi.org/10.1038/sj.cdd.4401682) PMID: [16247494](https://pubmed.ncbi.nlm.nih.gov/16247494/)
26. Liu Y, Liu XJ, Sun D. Ion transporters and ischemic mitochondrial dysfunction. *Cell Adh Migr.* 2009; 3(1): 94–98. PMID: [19276659](https://pubmed.ncbi.nlm.nih.gov/19276659/)
27. Lee WJ, Chien MH, Chow JM, Chang JL, Wen YC et al. (2015) Non-autophagic cytoplasmic vacuolation death induction in human PC-3M prostate cancer by curcumin through reactive oxygen species-mediated endoplasmic reticulum stress. *Sci Rep.*, 27(5): 10420.
28. Yoshida H, Matsui T, Yamamoto A, Okada T, Mori K(2001) XBP1 mRNA is induced by ATF6 and spliced by IRE1 in response to ER stress to produce a highly active transcription factor. *Cell.* 107(7), 881–91. PMID: [11779464](https://pubmed.ncbi.nlm.nih.gov/11779464/)
29. Okada K, Wangpoengtrakul C, Osawa T, Toyokuni S, Tanaka S, Uchida K. 4-Hydroxy-2-nonenal-mediated impairment of intracellular proteolysis during oxidative stress. Identification of proteasomes as target molecules. *J BiolChem.* 1999; 274(34):23787–23793.
30. Tang Y, Wang Y, Kiani MF, Wang B. Classification, Treatment Strategy, and Associated Drug Resistance in Breast Cancer. *Clin Breast Cancer.* 2016, S1526 8209(16)30108–2.